Use of Singular Value Decomposition to Characterize Age and Gender Differences in SPECT Cerebral Perfusion

Kenneth Jones, Keith A. Johnson, J. Alex Becker, Paul A. Spiers, Marilyn S. Albert and B. Leonard Holman
Departments of Psychiatry and Neurology, Massachusetts General Hospital, Boston; Departments of Radiology and Neurology, Brigham and Women's Hospital, Boston; Clinical Research Center, Massachusetts Institute of Technology, Cambridge; and Florence Heller School for Advanced Studies in Social Welfare, Brandeis University, Waltham, Massachusetts

The main objective of this study was to characterize changes in brain perfusion associated with normal aging and gender. **Methods:** Perfusion SPECT images using ^{99m}Tc-hexamethyl propyleneamine oxime (HMPAO) were obtained from 152 healthy subjects (67 men, 85 women) aged 50–92 yr. An automated method was developed to objectively assess image data from a large number of brain regions. Image data were reduced with singular value decomposition (SVD), which produced 20 eigenvectors capturing 97.05% of the total information content of 4320 regions from each subject. Subjects were scored individually on each vector. **Results:** Multivariate analyses demonstrated that there were no significant differences in whole-brain HMPAO uptake with age, but age-related regional declines were seen in lateral ventricular regions. Women had higher HMPAO uptake than men in estimates of global perfusion and regional perfusion in the midcingulate/corpus callosum, inferior temporal and inferior parietal areas. **Conclusion:** These discriminations demonstrate that singular value deomposition of SPECT data may be used to assess differences in perfusion patterns between groups of subjects. They replicate several previous findings, both with respect to age-related changes in perfusion and with respect to gender differences. In addition, they identify a previously unreported gender difference in biparietal regions.

Key Words: SPECT; technetium-99m-hexamethyl propyleneamine oxime; aging; gender differences

J Nucl Med 1998; 39:965–973

Normal aging results in detectable changes in brain structure and function. Numerous recent studies, using both CT and MRI have demonstrated there is an age-related decrease in brain size and an increase in cerebrospinal fluid space (*1–4*). There has been less agreement about the nature of the functional differences in brain metabolism with age. Using PET, some studies have reported focal alterations in metabolic rates but no evidence of an overall change with advancing age (*5–7*), while others report decreased metabolism overall (*8–10*) and in selected brain regions (*10–13*).

This study was undertaken to examine age-related differences in brain perfusion, using SPECT. While PET has a greater spatial resolution than SPECT, both measures are capable of demonstrating regional differences in perfusion. Because it was possible to obtain SPECT data from a substantial number of individuals for this study (152 subjects), we also examined gender differences.

Since we expected some of these differences to be difficult to detect, we developed an automated method of analyzing radiotracer uptake measured from a large number of brain regions and applied it to a large number of subjects. The purpose of the new method was to reduce the large volume of SPECT data, to analyze highly correlated data in an appropriate fashion, and to avoid capitalizing on chance in the analyses, all of which are challenges for data derived from functional imaging.

Received Apr. 23, 1997; revision accepted Oct. 9, 1997.
For correspondence or reprints contact: Marilyn Albert, MD, Massachusetts General Hospital, Psychiatry/Gerontology (149-9124), Bldg. 149 13th Street, Charlestown, MA 02129.

MATERIALS AND METHODS

Subjects

This study consisted of 152 (67 men, 85 women; age range 50–92 yr). The distribution of subjects across this age range was as follows: 50–55 yr = 10, 56–60 yr = 12, 61–65 yr = 10, 66–70 yr = 48, 71–75 yr = 47, 76–80 yr = 13, 80+ yr = 12. All subjects were right handed.

Subjects were recruited primarily through the print media and were screened first by a telephone interview. Subjects with a history of significant head trauma, neurological or psychiatric illness, major medical disease (e.g., diabetes, pulmonary disease) or use of medication with psychoactive properties (including certain classes of antihypertensives) were excluded. Subjects with mild medical conditions such as osteoporosis or arthritis were included.

All subjects considered appropriate for further evaluation received a physical, neurologic and psychiatric assessment. In addition, an EKG was performed and blood and urine specimens were analyzed to rule out evidence of occult disease (e.g., urinalysis, CBC). Any subject found to have a clinically significant abnormality based on this evaluation was excluded.

The potential participants also were administered a series of standardized cognitive tests to identify subjects with evidence of cognitive impairment. These included the vocabulary subtest of the Wechsler Adult Intelligence Scale, Revised (WAIS-R) (*14*), the Logical Memory Subtest of the Wechsler Memory Scale (WMS) (*15*), the Rey-Osterreith Complex Figure Test (*16*) and the Mini-Mental State Exam (MMSE) (*17*). Any subjects with scores on these tests that fell outside the normal range were eliminated. In addition, the majority of the subjects were followed for 3 yr and anyone who showed evidence of cognitive decline during that interval was eliminated from the study.

These criteria resulted in a sample that was not representative of the total population but rather of those individuals without evidence of major medical, neurologic or psychiatric disease. Table 1 presents the basic demographic and cognitive data pertaining to the participants.

Approximately half of the subjects were recruited through the Massachusetts Institute of Technology Clinical Research Center (*18*) and half were recruited through the Gerontology Research Unit of Massachusetts General Hospital. All participants signed informed consent statements for the study.

TABLE 1
Characteristics of the Study Sample

Gender	Number	Age (mean)	Age (s.d.)	Age (range)	MMSE (mean)
Male	67	70.34	7.96	50–92	29.26
Female	85	70.69	7.36	50–88	29.21
Total	152	70.55	7.59	50–92	29.23

MMSE = Mini-Mental State Exam.

SPECT Acquisition

All subjects (n = 152) were imaged using a digital dedicated brain imaging instrument (CERESPECT, Digital Scintigraphics, Inc., Waltham, MA) consisting of a stationary annular NAI crystal and rotating collimator system (*19*). The measured resolution using capillary line sources was 8.2 mm at center and 7.3 mm at 9 mm from center for ^{99m}Tc (*19–20*). Images were acquired 20 min after injection of 20.0 mCi (±1.0 mCi) ^{99m}Tc-HMPAO (Ceretec, Amersham Ltd., Amersham, UK) with the subjects supine at rest, eyes open, in a darkened room and with ambient white noise. Total acquisition time was 30 min.

Datasets were corrected for scatter and attenuation, reconstructed using filtered backprojection and displayed as a set of 64 slices (1.67-mm slice thickness) using a 128 × 128 matrix (1.66 × 1.66 × 2 mm pixels). Dataset anatomic orientation, surface contouring and scaling procedures were performed as detailed previously (*21*). Briefly, each dataset was oriented to a set of spatial reference standards, based on a modification of a standard atlas (*22*). The topmost slice representing activity from the thalamus was defined as a reference slice and 10 slices (thickness = 5 × 1.67 mm = 8.54 mm) were defined above and below the reference slice. Individual surface contouring accomplished scaling in x and y planes, compensating for brain size differences between subjects. A polar grid, consisting of spokes and contours, which was concentric with and the same shape as the external contour, was then superimposed on each summed slice. Forty-eight radial spokes and nine bands were generated for each dataset, forming 432 macrovoxels per slice, and more than 10 slices, 4320 macrovoxels per dataset.

Data Reduction of SPECT Information

This study used a technique known as singular value decomposition (SVD) to reduce the SPECT data from the 4320 macrovoxels mentioned above to 20 vectors which represented 97% of the variance. This method is described in detail below. These vectors then were used to examine differences in rCBF related to age and gender.

The SVD method can be considered an information-oriented technique since it uses principal components analysis procedures (PCA), a form of factor analysis, to concentrate information before examining the primary analytic issues of interest (*23–26*). The two most commonly used methods for analyzing SPECT and PET data use morphologically-based measures (*13,27*) or criterion oriented techniques, such as statistical parametric mapping (*28–29*). The relative strengths and weaknesses of these techniques have been discussed elsewhere (*30*). PCA has previously been applied to both PET and SPECT data (*31–33*), but with a slightly different analytic approach (i.e., measurements were made on brain regions that were identified a priori).

The SVD approach was selected for the present analysis because of its potential strengths in demonstrating results that are not related to a specific group difference (i.e., criterion value) or preselected morphological boundaries. It therefore seemed possible that it might reveal differences between groups not previously demonstrated by other techniques.

The first step in the analysis was to perform a z-score transformation of the data, by subtracting the sample mean from the value of each of the 4320 macrovoxels and dividing each resulting value by the standard deviation of the sample. The centered data then were divided by the square root of the sample size and subjected to a singular value decomposition (*23–26*). This reduced the data to its principal components. Although the SVD technique implicity analyzes the intervoxel correlation matrix, it does so by operating on the data matrix itself, rather than on the covariance matrix, and thus avoids the need to generate a matrix of more than 18 million correlations. The mathematics of the procedure have been previously described (*24*) and are briefly outlined in the Appendix.

In this study, the first 20 principal components generated by the SVD procedure were used. This number was chosen because the first 20 principal components captured 97.03% of the total data variance for the sample. The principal components, called SPECT vectors in this study, thus captured a substantial amount of the information in the original dataset.

The 20 vectors were rotated using the Varimax procedure (*34*). These rotated vectors retain the orthogonality of the original vectors, but allow the captured variance to be distributed from larger to smaller vectors, under the general rules of simple structure (*35*). The rotation neither adds to nor subtracts from the total information content of the vector ensemble, but merely redistributes the variance. These orthogonal vectors represent 20 independent association patterns of macrovoxel activity. They are nonredundant, orthogonal representations of individual differences in cerebral activity, as reflected by blood-flow activity common to all subjects. Thus each vector is a natural, functional combination of activity measures across macrovoxels that is independent of the information in the other vectors. That is, the macrovoxels are correlated within a vector, but the vectors are uncorrelated with one another. Table 2 presents some of the statistical characteristics of the vectors.

It should be noted that the vectors were not covaried for global or whole-brain counts. This decision was based on the fact that the macrovoxels are significantly spatially autocorrelated, and a covariance adjustment could conceivably delete important information. The absence of a correction for mean level means that each macrovoxel's perfusion contributes to the vectors. Thus, information about individual differences in overall perfusion rates are embedded in the vectors. To determine the consequences of this decision, a mean vector (i.e., a 21st vector) was created that permitted a direct examination of intraindividual differences in activity. The mean vector was developed by averaging the 4320 macrovoxels for each subject. Vector scores were then computed for each individual on each of the 21 vectors. The vector scores were used in all subsequent analyses.

The vector scores were calculated by multiplying the individual's perfusion in each of the 4320 macrovoxels by the weights for

TABLE 2
Characteristics of the SPECT Vectors After Varimax Rotation

Vector	Sum of squares	Variance for rotated loadings (%)	Average loading factor	Maximum loading	Minimum loading	Vector number
V01	2648.39	61.31	0.10	0.90	0.77	Vector V01
V02	976.95	22.61	0.26	0.90	0.46	Vector V02
V03	313.15	7.25	0.00	0.79	0.25	Vector V03
V04	22.78	0.53	−0.20	0.43	0.03	Vector V04
V05	28.49	0.66	−0.23	0.62	0.04	Vector V05
V06	18.03	0.42	−0.13	0.27	0.02	Vector V06
V07	30.77	0.71	−0.17	0.48	0.06	Vector V07
V08	25.27	0.58	−0.20	0.52	0.05	Vector V08
V09	9.34	0.22	−0.13	0.30	0.01	Vector V09
V10	14.79	0.34	−0.16	0.40	0.02	Vector V10
V11	16.79	0.39	−0.20	0.18	0.01	Vector V11
V12	11.19	0.26	−0.19	0.24	0.02	Vector V12
V13	15.71	0.36	−0.22	0.44	0.01	Vector V13
V14	7.65	0.18	−0.20	0.19	0.01	Vector V14
V15	7.08	0.16	−0.10	0.17	0.01	Vector V15
V16	8.35	0.19	−0.12	0.28	0.01	Vector V16
V17	15.08	0.35	−0.11	0.26	0.03	Vector V17
V18	8.17	0.19	−0.21	0.16	0.00	Vector V18
V19	7.12	0.16	−0.18	0.18	0.01	Vector V19
V20	6.80	0.16	−0.17	0.35	0.01	Vector V20
Total	4191.88	97.03				

the normative sample, and summing them to form a linear weighted sum (the resultant vector scores are z transformed as a result of this procedure). Since there were 21 vectors for the normative sample, each individual had 21 vector scores.

Statistical Analysis

The distribution of the SPECT data was examined to establish that parametric data analysis procedures were appropriate. SPECT vector 21, which represented the mean perfusion rates of the subjects, was analyzed with analysis of variance (ANOVA) to examine differences with age and gender. For these analyses, the subjects were divided into two age groups, using 72 yr as the cutoff point. There were 90 subjects under the age of 72 yr and 62 subjects who were 72 yr and over.

Then SPECT vectors 1–20 were analyzed. First, multivariate analysis of variance (MANOVA) was used to evaluate the manner in which SPECT vectors 1–20 varied with age and gender, with the same grouping strategy as for the ANOVA. To examine age effects, with age treated as a continuous variable, linear multipile regression analysis was performed. Discriminant function analysis also was used to examine differences among the subjects based on age and gender. Finally, MANOVA was used to determine whether the primary findings relating to age and gender differed on the basis of the site at which the subjects had been recruited.

Backprojection of Discriminating SPECT Data

To facilitate the interpretation of the SPECT vectors, a method of backprojecting the vectors that discriminated the groups was developed that produced a map of the cerebral location of the macrovoxels that contributed to each discrimination. To accomplish this, the 20 discriminant weights derived from the discriminant function analyses (described below) were multiplied by the matrix of the vector loadings from the normative sample. This yielded 4320 elements (actually correlations of each macrovoxel with the discriminant score). An iterative surface matching algorithm then was used to generate a rigid body transformation of the SPECT data on MRIs from five different subjects with differing degrees of atrophy. Each MRI was scaled to the Tailarach coordinate system (*22*). All regions that had factor loadings greater than 0.20 were examined and the loading levels were displayed in color. The superimposed images were reviewed in detail by a physician with special expertise in neuroimaging. The brain regions were labeled, based on those that were consistently identified across the set of MRI images and Tailarach coordinates were provided (*22*). All vectors were used for the backprojections, but were weighted proportionate to their ability to discriminate. Thus, the SPECT data were used to display the macrovoxels throughout the brain, in terms of the differences among the groups.

It should be emphasized that this backprojection was not itself a method of discriminating the groups, but rather a method of portraying the group differences that had been established by discriminant function. Likewise, the vectors themselves were not labeled because the primary goal was to develop a method of combining them for the purposes of discrimination. Thus, the figures below represent the brain regions that were identified by combining all significant vectors that contributed to a particular group discrimination.

RESULTS

Differences in SPECT Perfusion with Age

The multiway ANOVA of the SPECT mean vector (i.e., the 21st vector) demonstrated no significant difference with age in the mean perfusion rate of the subjects ($F(1, 140) = 0.01$; $p = 0.99$). There also were no significant interaction effects.

A three-way MANOVA was then performed in which the subjects were stratified by age (i.e., all subjects less than 72 yr in one group and all subjects 72 yr or greater in another), gender and nature of recruitment. In the MANOVA the 20 vector scores (from vectors 1–20) were entered as dependent variables simultaneously and each interaction term was tested for statistical significance.

There was a highly significant effect for age ($F(20, 112) = 2.80$; $p \leq 0.0001$) and gender ($F(20, 121) = 3.20$; $p \leq 0.0001$). However, there were no significant interaction effects, indicating that the age and gender effects did not vary significantly with the site at which the sample was recruited.

To examine the age effect for vectors 1–20 more closely, a linear regression was performed in which age was treated as a continuous variable. Table 3 presents the results of this regression. In this regression gender was introduced as a control variable, but its effect was negligible (i.e., beta = −0.03; t =

TABLE 3
Multiple Regression of Vectors 1–20 with Age

Vector	Beta	r^2	t	p value
V14	0.38	0.27	4.35	0.0001
V01	0.35	0.21	3.73	0.0003
V17	0.27	0.16	3.19	0.0018
V05	−0.27	−0.08	−3.13	0.0022
V18	0.21	−0.01	2.40	0.0176
V13	−0.21	−0.33	−2.25	0.0260
V16	0.18	0.11	2.09	0.0388
V12	−0.16	−0.10	−1.97	0.0500
V03	−0.16	−0.12	−1.96	0.0500
V08	0.18	0.04	1.89	0.0611
V04	−0.13	−0.20	−1.50	0.1349
V20	0.13	0.01	1.50	0.1356
V07	−0.14	−0.10	−1.41	0.1604
V06	−0.10	0.04	−1.23	0.2227
V09	−0.10	−0.03	−1.03	0.3046
V11	−0.06	0.14	−0.71	0.4816
V19	−0.04	0.09	−0.43	0.6671
V02	−0.03	−0.07	−0.35	0.7281
V15	0.02	0.11	0.25	0.8054
V10	0.02	0.03	0.15	0.8812
R		0.64		
R-sq		0.41		
F-ratio		4.2		
df1		21		
df2		130		
p <		0.0001		

−0.36; p = 0.72). The results indicated a significant linear relationship between the SPECT vectors and age (r = 0.64; R^2 = 0.41; F = 4.22; df = 21,130; p < 0.0001).

A discriminant function was computed to determine the degree to which the subject's age group could be correctly identified based on SPECT vectors 1–20 (i.e., < 72 yr versus ≥ 72 yr). The overall classification rate for the function, using equal apriori weights, was 76.9% and it was significant (Table 4). The associated multiple correlation was 0.56. Four vectors were significant at the 5% level or greater. Together, these results indicate that the 20-vector ensemble contained significant discriminatory information with regard to age. Table 4 gives the parameters and their statistical significances for the two-age level discriminant function. The weights are the standardized discriminant function weights. The loadings are the correlations of the vector variable with the discriminant score. The correlations are the correlation with the vector and the dummy variable defining group. The t-values represent the significance level associated with each weight.

An examination of the backprojections of the discriminant scores from the significant discriminant functions indicated that age-related differences primarily pertained to alterations in ventricular size. This was particularly striking in Vectors 2 and 3. This age-related difference is shown graphically in Figure 1. In this figure, the SPECT data were overlaid on a typical MRI scan. The anatomical label assigned to the region was based on the examination of the overlay on mulitiple MRI exemplars and on the location of the SPECT region that was most statistically significant. The significant differences between the groups were highest

TABLE 4
Discriminant Function Analysis Using SPECT Vectors to Predict Age Group (< 72 vs. ≥ 72)

Vector	Beta	Load	r^2	t	p value
V14	0.66	0.34	0.22	3.32	0.0012
V17	0.47	0.19	0.12	2.40	0.0180
V02	−0.39	−0.26	−0.17	−2.06	0.0419
V12	−0.36	−0.20	−0.13	−1.96	0.0500
V05	−0.37	−0.05	−0.03	−1.84	0.0679
V01	0.38	0.31	0.20	1.80	0.0740
V03	−0.34	−0.18	−0.12	−1.76	0.0813
V13	−0.34	−0.46	−0.30	−1.62	0.1067
V08	0.33	0.17	0.11	1.52	0.1316
V07	−0.34	−0.18	−0.12	−1.47	0.1447
V09	−0.29	−0.07	−0.05	−1.31	0.1918
V20	0.19	−0.01	0.00	0.94	0.3472
V10	0.18	0.03	0.02	0.75	0.4547
V16	0.15	0.02	0.02	0.74	0.4632
V19	0.15	0.23	0.15	0.72	0.4752
V18	0.13	−0.15	−0.10	0.65	0.5183
V15	0.04	0.03	0.02	0.23	0.8206
V06	−0.04	0.12	0.08	−0.22	0.8264
V04	0.03	−0.12	−0.08	0.17	0.8631
V11	0.01	0.22	0.15	0.07	0.9422
R		0.56			
R-sq		0.31			
F-ratio		2.79			
df1		20			
df2		121			
p<		0.0001			
% Correct					
≤ 71 yr		72.60%			
> 72 yr		80.00%			
Overall		76.90%			

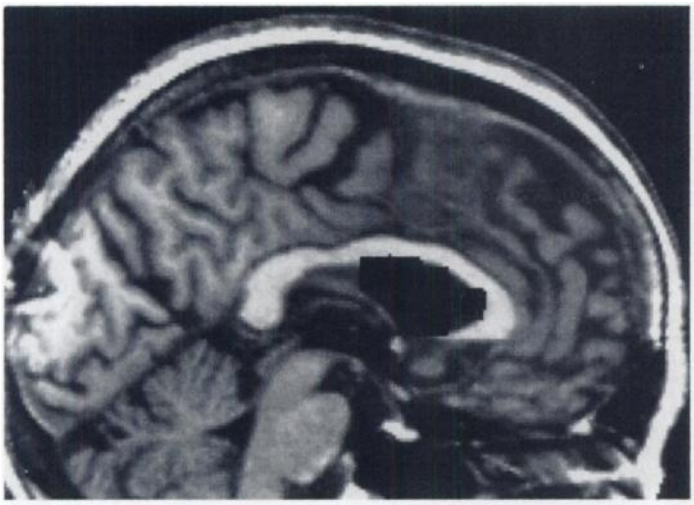

FIGURE 1. This figure represents the ventricular areas that differ between the subjects on the basis of age. All significant vectors, as shown in Table 4, contributed to the age group discrimination. The significant differences between the two age groups were highest (i.e., most decreased in older subjects compared to younger ones) within the region that is the darkest and lowest in the lighter areas.

(i.e., most decreased in older subjects compared to younger ones) within the region that is the darkest and lowest in the lighter areas.

Differences in SPECT Perfusion by Gender

The analysis of the SPECT mean vector (i.e., the 21st vector) by ANOVA demonstrated a significant difference between the genders in the mean perfusion rate of the subjects ($F(1, 140) = 13.7$, $p \leq 0.0001$). There was no significant interaction with the age of the subjects ($F(1, 140) = 0.65$, $p = 0.52$).

A discriminant function analysis then was performed with Vectors 1–20 to determine whether there were significant differences between the genders. The overall classification rate for the function, using equal a priori weights, was 75.7% and it was significant. The associated multiple correlation was 0.59. Seven vectors were significant at the 5% level or greater. Together, these results indicate that the 20-vector ensemble contains significant discriminatory information with regard to gender. Table 5 gives parameters and their statistical significances for the two-gender level discriminant function. The weights are the standardized discriminant function weights. The loadings are the correlations of the vector variable with the discriminant score. The correlations are the correlation with the vector and the dummy variable defining group. The t-values represent the significance level associated with each weight.

Figures 2-4 represent backprojections of the discriminant function representing the differences between the genders. The data are overlaid on a typical MRI in sagittal section to display the anatomical sources of the discriminating information. The primary regional differences in rCBF between the genders included higher rCBF levels in the women compared to the men in the region of the mid cingulate/corpus callosum, the inferior temporal lobe on the right, and the inferior parietal lobe bilaterally (centered at $\pm$ x = 30, y = −40, z = −40). The SPECT data are overlaid on a typical MRI scan. The significant

TABLE 5
Discriminant Function Analysis Using SPECT Vectors to Predict Gender*

Vector	Beta	Load	r^2	t	p value
V02	0.83	0.39	0.27	5.11	0.0001
V12	−0.48	−0.21	−0.15	−2.76	0.0067
V11	0.46	0.37	0.26	2.47	0.0148
V06	0.45	0.14	0.10	2.43	0.0163
V01	0.51	0.21	0.15	2.40	0.0179
V16	0.41	0.09	0.07	2.18	0.0314
V08	0.42	0.12	0.09	2.05	0.0421
V15	−0.31	−0.17	−0.12	−1.83	0.0703
V10	−0.39	0.01	0.01	−1.71	0.0904
V03	0.31	0.16	0.12	1.68	0.0964
V20	0.26	0.15	0.10	1.34	0.1834
V05	0.22	0.06	0.04	1.09	0.2768
V07	0.23	−0.02	−0.02	1.03	0.3064
V19	−0.16	0.02	0.02	−0.79	0.4285
V18	−0.11	−0.06	−0.04	−0.58	0.5621
V14	−0.12	−0.02	−0.01	−0.57	0.5727
V04	−0.09	0.03	0.02	−0.46	0.6452
V09	−0.09	0.00	0.00	−0.45	0.6557
Age	−0.07	0.00	0.00	−0.36	0.7201
V13	0.07	−0.05	−0.03	0.34	0.7324
V17	−0.04	−0.07	−0.05	−0.23	0.8219
R		0.59			
R-sq		0.35			
F-ratio		3.2			
df1		20			
df2		121			
p<		0.0001			
% Correct					
Males		85.10%			
Females		68.20%			
Overall		75.70%			

*Male = 1; female = 2.

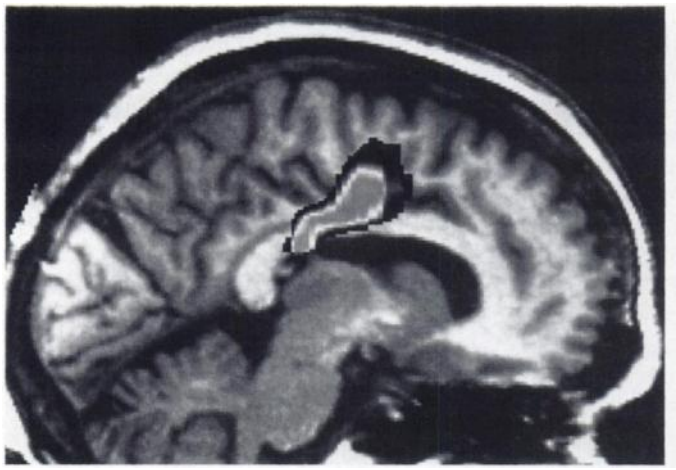

FIGURE 2. This figure represents the midcingulate/corpus callosal area that differed between the genders. All significant vectors, as shown in Table 5, contributed to the group discrimination. Figures 3 and 4 also demonstrate regions that differed between the genders. Three separate figures are used to portray the group differences because the significant regions are anatomically distributed and difficult to show clearly on one figure. The significant differences between the genders were highest (i.e., most increased in women compared to men) within the region that is at the lighter end of the spectrum and lowest within the region that is darkest.

differences between the groups were highest (i.e., most increased in women compared to men) within the region that is at the lighter end of the spectrum and lowest within the region that is darkest.

A separate analysis, in which the SPECT vectors were established separately on men and women (data not shown) indicated that the intercorrelation of the vector scores for men and women was more than 75%. (In this latter instance, the SPECT vectors were calculated in the same manner described above, with the exception that the principal components were calculated separately for the men and the women, thus permitting one to correlate the SPECT scores for the two groups with one another).

Replication of Results

The prediction equations developed on the subjects described above were tested for replicability on another sample of 62 (22 men, 40 women). The age function classified 67% of the second sample correctly into younger (age $\leq$ 71 yr) and older (age $>$ 71 yr) individuals (chi square = 6.6, df = 1, $p < 0.01$) (NB: the accuracy for the original sample was 76.9%). The gender discriminant function classified 70% of the second sample correctly (versus 75.7% accuracy for the original sample).

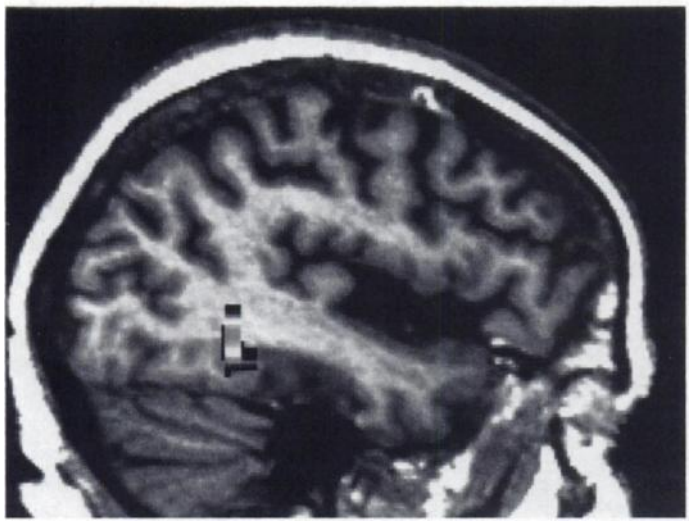

FIGURE 3. This figure represents the right inferior temporal region that differs between the genders. All significant vectors, as shown in Table 5, contributed to the group discrimination. Figures 2 and 4 also demonstrate regions that differed between the genders. They are portrayed on three separate figures because the regions are distributed anatomically and are difficult to show clearly on one figure.

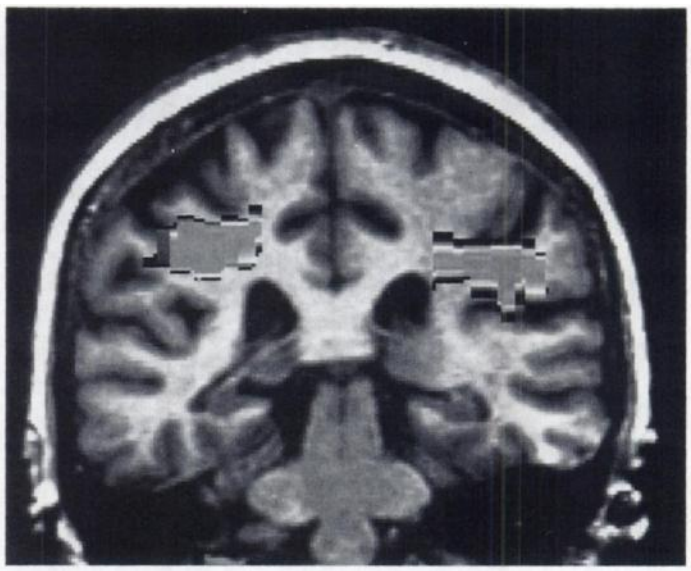

FIGURE 4. This figure represents the bilateral inferior parietal regions that differ between the genders. All significant vectors, as shown in Table 5, contributed the group discrimination. Figures 2 and 3 also demonstrate regions that differed between the genders. They are portrayed on three separate figures because the regions are anatomically distributed and difficult to show clearly on one figure.

DISCUSSION

These results indicate that subjects 50 yr of age and over do not demonstrate a significant overall decline in rCBF with advancing age. There is, however, a regional rCBF difference, primarily evident in the ventricular regions. These findings are consistent with several previous reports using PET (*9–13*). Studies that have reported an overall decline in rCBF with age have generally included subjects in their 20s through 40s (*8–10*).

In addition, differences in rCBF between the genders were evident. These differences did not interact with age, but rather pertained to consistent differences between genders across the age range examined. There was a generally higher perfusion rate among the women. This is consistent with previous studies of CBF (*36–37*), but contrasts with most previous studies of glucose metabolism (*8,10*).

There also was evidence of some differences in rCBF between the genders that were regional, primarily evident in the area of the right mid cingulate/mid corpus callosum, the right inferior temporal lobe and the inferior parietal lobe bilaterally. Differences between the genders previously have been reported in the region of the cingulate/corpus callosum (*36*) and the temporal lobe (*10,33,36*). Gender differences in parietal lobe perfusion have not, to our knowledge, previously been described. There were, nevertheless, more similarities than differences between the genders, as the intercorrelation of vectors calculated separately for men and women was over 75%.

The results presented above must be considered in light of the potential limitations of the study. The first pertains to the generalizability of the findings. The study sample was screened quite thoroughly to be free of any evidence of major disease. These screening procedures have the effect of restricting the range of the data and thus reducing the correlations in the

sample (*38*). This, in turn, means that Type II error is increased and power is reduced. Mitigating these effects is the size of the sample, which is substantial, and the fact that highly significant effects were found.

The second potential limitation pertains to issues related to the SPECT technique itself. SPECT has less spatial resolution than PET and thus fine distinctions regarding differences within regions are not possible. Moreover, in this study regions were not defined a priori, thus it may be possible that additional regional differences would be evident if regions of interest were drawn and SPECT perfusion then measured within a given region, work that is currently underway. However, the fact that these findings replicate many of those previously reported using PET suggest that the present results are likely to be valid.

It should also be pointed out that the method of surface contouring used to adjust for individual differences in brain size used here, reduced the influence of atrophy at the boundary between the cortex and subarachnoid space. Thus, the SPECT measurements in cortex are likely to be primarily derived from perfusion of brain, rather than a result of averaging brain and CSF. However, contouring was not applied to ventricular regions. Therefore, some of the SPECT vectors pertained to differences in ventricular size and reflected age-related alterations in these regions, confirming numerous previous findings. To fully evaluate the contribution of atrophy, MRI registration and volumetric correction of SPECT data would be required, and was not possible in our study because MRIs were not available in all subjects.

Lastly, one must consider a methodological issue raised by this study. This pertains to the treatment of the individual global mean perfusion, which is somewhat different than that of prior studies (*28,31–32*). Various suggestions for the treatment of the global mean have been proposed; they have included dividing all regional values by the mean, creating a ratio between each voxel and a representative region such as the cerebellum, and treating the mean rCBF as a covariate. Each of these has merit in particular situations. The present analysis examined issues related to the global mean perfusion rate in two ways. It was examined directly, by means of the mean vector (i.e., the 21st vector), as described above. In addition, the global mean was incorporated into the 20 vectors by means of the Varimax rotation. This made it possible to explore the degree to which an individual's perfusion rate was distributed across the vectors and thus contributed to the group differences being examined. An examination of the intercorrelation matrix of the 21 vectors indicated that global mean perfusion rate was strongly correlated with vectors 1 through 3 (r^2 = 0.84, 0.36, 0.39, respectively). However, there was considerable additional information in these vectors. Thus, for example, vector 1 was significantly related to age ($p \leq 0.0003$) but this relationship did not derive from an age-related decline in overall mean perfusion, since this was not seen when examined directly.

CONCLUSION

These findings demonstrate that the SVD approach to SPECT data analysis (which utilizes parsimonious statistical tests of significance and is not based on multiple criterion oriented statistical tests) can lead to meaningful discriminations between groups of subjects. They replicate several previous findings, both with respect to age-related changes in perfusion and with respect to gender differences. In addition, they identify a previously unreported gender difference in biparietal regions. This may be related to numerous reports that men tend to perform better than women on nonverbal tasks (*39*) and can be explored in future analyses.

ACKNOWLEDGMENTS

This research was supported by National Institute on Aging Grant P01-AG04953, the Massachusetts Institute of Technology Center for Brain Scienes and Metabolism Charitable Trust and National Institute of Health GCRC Grant M01RR00088. We thank Dr. Mary Hyde for her invaluable assistance with data management and programming.

APPENDIX

Principal Components Analysis

The SPECT analyses described in this manuscript are based on principal components analysis (PCA) (*40*). Hotelling is usually seen as the formulator of the modern procedure of PCA. The theorem, which has been rediscovered many times, is proved in Eckart (*41*). It shows that any real matrix may be transformed into a set of left vectors (P), a set of right vectors (Q′) and a diagonal matrix of roots (L). The continued product of these matrices exactly reproduces the observed data (Z):

$$Z = PLQ'. \qquad \text{Eq. 1}$$

If the raw (observed) data matrix, X, represents n rows of observations by m columns of variables, is standardized so that each variable has a zero mean and a unit variance, and we further scale this by dividing each element by the square root of the number of cases, this new matrix, Z, when premultiplied by its transpose will form the matrix of variable intercorrelations:

$$R = Z'Z = QLP'PLQ' = QL^2Q'. \qquad \text{Eq. 2}$$

Because P is orthonormal, when multiplied by its transpose an identity matrix result. This is the correlational form of the Eckart-Young Theorem and is sometimes written as:

$$R = FF',$$

where:

$$F = QL.$$

The columns of F are the well-known component loadings which describe the correlation between each observed variable and the latent variable component score. It is often the case that fewer latent variables are retained than the maximum needed to exactly reproduce the correlation matrix. In this situation the correlation matrix is only approximately reproduced. If the carat represents approximation, then:

$$\hat{R} = \hat{F}\hat{F}'.$$

Bartlett's (*42*) test of significance may be used to determine the adequacy of the approximation of R.

Singular Value Decomposition

There are several methods for finding the latent roots and vectors of the data matrix that results from the above procedures. In the usual case where there are more observations than variables (i.e., $n > m$), it is more efficient to generate an associated matrix, as the correlation matrix, and to use Equation 2. However, when the number of variables is very large and the number of cases modest, the computer resources needed to solve Equation 2 may be prohibitive.

One solution to this problem is to solve Equation 1 directly. This is known as the singular value decomposition technique (SVD) (*22,23*). The number of nonzero latent variables (roots) can be no larger than n or m, whichever is the smaller. If the data are centered, by subtracting the mean from each value, then it is $n - 1$ or m whichever is the smaller.

If we have a set of measures (e.g., regional cerebral blood flow measures within each macrovoxel), we may compute the

linear function of these values, which represents the first principal component. There are three common forms of the scores: the raw data as gathered, the mean centered data, or the standardized data which is the mean centered data divided by the standard deviation of the sample. The latter is used in the present analyses. If these scores are scaled by dividing by the square root of the number of cases, we have the *n*-rowed by *m*-columned matrix Z:

$$R = Z'Z = QL^2Q'.$$

The L-square represent the so-called latent roots or eigenvalues of the matrix R and:

$$Z = PLQ'.$$

As Z is an *n*-by-*m* matrix so is PLQ' and we can get Q without forming the large *m*-by-*m* matrix. A smaller number of components may then be selected that account for a substantial portion of the total variance (information). The resultant vectors may then be rotated to simple structure (*34*). In addition, the Q vectors may be used to compute component scores for each member of the sample or subjects outside the analytical sample, The component scores are just the projections of each subject's score vector on the component axes. If *k* axes are retained, *k* scores will be computed, *k* being less than *m*. As the Q vectors are the direction cosines between the variable vectors and the components, the P vectors are the direction cosines between the subject vectors and the components. In one standardization or another these are the component scores. In standard form these scores will be:

$$S = \sqrt{n}ZQL^{-1} = \sqrt{n}P$$

$$(n * k) = (n * m)(m * k)(k * k).$$

Here *k* is the number of retained components. The matrix of components scores, standardized to unit variance and zero mean, may then be used to stand for the information contained in the *m* original data scores. These scores are orthogonal to one another, hence represent independent contributions to whatever criterion they are used to predict. The above may be rewriten as:

$$S = XF(F'F)^{-1},$$

$$s_{ik} = \sum_{j=1}^{m} c_j x_{ij},$$

where *m* is the number of variables, *i* and *k* represent the individual and *k* the vector component. The *c*s are the so-called score coefficients which are the entries of FL^{-2}.

In the present analysis 20 latent roots or vectors were retained, which accounted for 97.03% of the total variance in the 4320 SPECT macrovoxels.

Varimax Rotation

Thurstone proposed a set of rules for judging whether a set of latent variables are satisfactorily described by the observed variables (*34*). According to these procedures, it is both legitimate and desirable to refine the latent variables generated by PCA by further rotation of the component axes to achieve simple structure. Basically this involves taking variance from the larger components and distributing it to other components in such a manner as to enhance interpretability. One way to accomplish this is with the Varimax procedure (*33,43*). When there is a rotation of the loading matrix, F, the scores may be estimated by several alternative procedures, the most common of which is the regression method. This is the method that was used in the present manuscript after a Varimax rotation to simple structure.

In equation form the rotation is simply:

$$B = FT.$$

Here B is an *m*-by-*k* matrix of rotated loadings, F is the original *m*-by-*k* principal component loadings and T is the *k*-by-*k* orthogonal transformation matrix derived by the Varimax analytical procedure. The matrix B is the orthogonal since it results from the multiplication of two orthogonal matrices. It contains no less nor more information than was in the original matrix, F, but the information is redistributed to conform to the rules of simple structure. If one had no interest in interpreting the individual vectors then rotation would be unnecessary as the prediction of the entire set of latent variables (e.g., the 20 SPECT vectors) for any given dependent variable would be the same whether rotated or unrotated. A similar set of rotated scores may be computed from:

$$V = XB(B'B)^{-1}.$$

These scores may be used to predict a dependent criterion.

Backprojection of Discriminating Data

A method of backprojecting the rotated vectors onto the cerebral locations of the macrovoxels was developed for the present study to identify the brain regions implicated by the analyses. For example, if one discovers some linear combination of vector scores which optimally and significantly predict a continuous criterion, as in a regression model, or group membership, as in a discriminant model, then one may apply the derived beta weights or standardized discriminant weights to the vector scores to compute a composite score of best prediction. Thus, if the discriminant score be known as *d*, and is a linear function of the vector scores, V, Then:

$$d_i = \sum_{j=1}^{m} \beta_j v_{ij}.$$

Here the betas are the optimized weights and the *v*s are the vector scores. In matrix notation this is:

$$d = V\beta'.$$

The loadings (i.e., correlations) for the original (macrovoxel) variables on the transformed scores are the correlations for the *d* scores with the original, X, scores.

$$R_l = \frac{d'X}{N\sigma_d}.$$

Here we assume that each of the scores in the matrix X has unit variance, but *d* need not. By substitution of appropriate above formulae in this equation we may derive a simple expression for the backprojection of the *d* scores onto the original macrovoxels, X;

$$R_l = \frac{\beta V'X}{N\sigma_d} = \frac{\beta(B'B)^{-1}B'X'X}{N\sigma_d}$$

$$R_l = \frac{\beta(T'F'FT)^{-1}T'F'X'X}{N\sigma_d} = \frac{\beta(T'L^2T)^{-1}T'F'FF'(N)}{N\sigma_d}$$

$$R_l = \frac{\beta(T'L^2T)^{-1}T'F'L^2}{\sigma_d} = \frac{\beta T'F'}{\sigma_d} = \frac{\beta B'}{\sigma_d}.$$

The rotated loadings are premultiplied by the appropriate weights (betas), to yield a set of correlations, in this case, for

each of the 4320 macrovoxels with the particular score of prediction. The betas are of order 1 by 20, the rotated loadings, B-prime, in the present analyses. The values of these loadings (correlations) represent the degree to which (positively or negatively) a given macrovoxel defines a high score on the *d* variable. If these are plotted on the original map they portray a profile of high scores. When these are overlaid on a typical MRI one may determine the general anatomical areas which are contributing most to *d*, hence defining it.

REFERENCES

1. Zatz L, Jernigan T, Ahumada A. Changes in computed cranial tomography with aging: intracranial fluid volume. *Am J Neurorad* 1982;3:1–11.
2. Stafford J, Albert M, Naeser M, Sandor T, Garvey A. Age-related differences in computed tomographic scan measurements. *Arch Neurol* 1988;45:405–419.
3. Jernigan T, Archibald S, Berhow M, Sowell E, Foster D, Hesselink J. Cerebral structure on MRI I: localization of age-related changes. *Biol Psychiat* 1991;29:55–67.
4. Matsumae M, Kikinis R, Morocz I, et al. Age-related change in intracranial volumes in normal adults assessed by MRI. *J Neurosurg* 1996;84:982–991.
5. Duara R, Margolin R, Robertson-Tchabo E, et al. Cerebral glucose utilization, as measured with positron emission tomography in 21 resting healthy men between the age of 21 and 83 years. *Brain* 1983;106:761–775.
6. DeLeon M, George A, Tomanelli J, et al. Positron emission tomography studies of normal aging, a replication of PET III and 18-FDG using PET IV and 11-CDG. *Neurobiol Aging* 1987;8:319–323.
7. Martin A, Friston K, Colebatch J, Frackowiak R. Decreases in regional cerebral blood flow with normal aging. *J Cereb Blood Flow Metab* 1991;4:684–689.
8. Kuhl D, Metter E, Riege W, et al. Effect of human aging on patterns of regional glucose metabolism as assessed by ^{18}F positron emission tomography. *J Cereb Blood Flow Metab* 1982;2:163–171.
9. Yoshii F, Barker W, Chang J, et al. Sensitivity of glucose metabolism to age, gender, brain volume, brain atrophy, and cerebrovascular risk factors. *J Cereb Blood Flow Metab* 1988;8:654–661.
10. Murphy D, DeCarli C, McIntosh A, et al. Sex differences in magnetic resonance imaging and positron emission tomography study on the effect of aging. *Arch Gen Psychiatr* 1996;53:585–594.
11. Chawluk J, Alavi A, Dann R, et al. Positron emission tomography in aging and dementia: the effect of cerebral atrophy. *J Nucl Med* 1987;28:431–437.
12. Alavi A. The aging brain. *J Neuropsychiatry* 1989;1:S51–S56.
13. Loessner A, Alavi A, Lewandrowski K, et al. Regional cerebral function determined by FDG-PET in healthy volunteers: normal patterns and changes with age. *J Nucl Med* 1995;36:1141–1149.
14. Wechsler D. *The Wechsler adult intelligence scale-revised.* New York: Psychological Corporation; 1981.
15. Wechsler D. A standardized memory scale for clinical use. *J Psychol* 1945;19:87–95.
16. Rey A. L'Examen psychologique dans les cas d'encephalopathie tramatique. *Arch Psychol* 1941;28:286–340.
17. Folstein MF, Folstein SE, McHugh PR. Mini-mental state. A practical method for grading the cognitive state of patients for the clinician. *J Psychiat Res* 1975;12:189–198.
18. Spiers P, Myers D, Hochanadel G, Lieberman H, Wurtmen RJ. Citicoline improves verbal memory in aging. *Arch Neurol* 1996;53:441–448.
19. Genna S, Smith A. The development of ASPECT, an annular single crystal brain camera for high efficiency SPECT. *IEEE Trans Nucl Sci* 1988;35:654–658.
20. Holman B, Carvalho P, Zimmerman R, et al. Brain perfusion SPECT using an annular single crystal camera: initial clinical experience. *J Nucl Med* 1990;31:1456–1561.
21. Johnson K, Kijewski M, Becker J, et al. Quantitative brain SPECT in Alzheimer's disease and normal aging. *J Nucl Med* 1993;34:1–5.
22. Tailarach J, Tournoux P. *Co-planar stereotaxic atlas of the human brain.* New York: Thieme Medical Publishers; 1988.
23. Golub G, Kahane W. Calculating the singular values and pseudo-inverse of a matrix. *SIAM J of Num Anal* 1965;2:205–224.
24. Golub G, VanLoan C. *Matrix computations*, 2nd ed. Baltimore: Johns Hopkins University Press; 1989.
25. Jones K. Relation of R-analysis factor scores to Q-analysis factor loadings. *Psych Rep* 1967;20:247–249.
26. Jones K, Duffy F, Albert M. The principal components reduction of very large numbers of brain electrical activity variables to orthogonal aactors. *Proceedings of the Joint Statistical Meetings, American Statistical Assn.* Boston: American Statistical Association; 1992.
27. Holman BL, Johnson K, Basem G, et al. The scintographic appearance of Alzheimer's disease: a prospective study using technetium-99m-HMPAO SPECT. *J Nucl Med* 1992;33:181–185.
28. Friston K, Frith C, Liddle P, Frackowiak R. Comparing functional PET images: the assessment of significant change. *J Cereb Blood Flow Metab* 1991;11:690–699.
29. Jagust W. Functional imaging patterns in Alzheimer's disease. *Annal NY Acad Sci* 1996;777:30–36.
30. Ford I, McColl J, McCormack A, McCrory G. Statistical issues in the analysis of neuroimages. *J Cereb Blood Flow Metab* 1991;11:A89–A95.
31. Clark C, Carson R, Kessler R, et al. Alternative statistical models for the examination of clinical positron emission tomomography fluordeoxyglucose data. *J Cereb Blood Flow Metabol* 1985;5:142–150.
32. Strother S, Kanno I, Rottenberg D. Principal component analysis, variance partitioning, and 'functional connectivity'. *J Cereb Blood Flow Metab* 1995;15:353–360.
33. Houston A, Kemp P, MacLeod M. A method for assessing the significance of abnormalities in HMPAO SPECT images. *J Nucl Med* 1994;35:239–244.
34. Kaiser H. The varimax criterion for analytic rotation in factor analysis. *Psychometrika* 1958;23:187–200.
35. Thurstone LL. *Multiple factor analysis.* Chicago: University of Chicago Press; 1947.
36. Gur R, Mozley L, Mozley P, et al. Sex differences in regional cerebral glucose metabolism during a resting state. *Science* 1995;267:528–531.
37. Devous M, Stokely E, Chehabi H, Bonte F. Normal distribution of regional cerebral blood flow measured by dynamic single-photon emission tomography. *J Cereb Blood Flow Metab* 1986;6:95–104.
38. Carroll J. The nature of the data–or how to choose a correlation coefficient. *Psychometrika* 1961;26:347–372.
39. Wiederholdt W, Cahn D, Butters N, Salmon D, Kritz-Silverstein D, Barrett-Connor E. Effects of age, gender and education on selected neuropsychological tests in an elderly community cohort. *J Am Geriatr Soc* 1993;41:639–647.
40. Hotelling H. Analysis of a complex of statistical variables into principal components. *J Ed Psych* 1933;24:417–441, 498–520.
41. Eckart C, Young G. The approximation of one matrix by another of lower rank. *Psychometrika* 1936;3:211–218.
42. Bartlett MS. Tests of significance in factor analysis. *Brit J Stat Psych* 1950;3:77–85.
43. Kaiser HF. Computer program for Varimax rotation in factor analysis. *Ed Psych Measmt* 1959;19:413–420.